Passage of high-energy partons through a quark-gluon plasma

Yuji Koike
Department of Physics and Astronomy, University of Maryland, College Park, Maryland 20742

T. Matsui
Nuclear Theory Center and Physics Department, Indiana University, Bloomington, Indiana 47405 and Center for Theoretical Physics, Laboratory for Nuclear Science and Department of Physics, Massachusetts Institute of Technology, Cambridge, Massachusetts 02139*
(Received 13 November 1991)

We discuss the energy loss of a colored particle ($\sim$ a leading particle of jets) and a color dipole ($\sim$ heavy quarkonia) passing through a quark-gluon plasma (QGP) taking into account the dynamic screening effect, in the framework of the semiclassical kinetic theory. We also show how the energy supplied by these test charges is distributed in the QGP, which gives us further physical insight about the energy-loss mechanism and the plasma response to such external probes.

PACS number(s): 12.38.Mh, 12.38.Bx, 25.75.+r

I. INTRODUCTION

The energy loss of a fast charged particle passing through matter is a classic problem in electrodynamics [1,2] and of special importance in plasma physics where one can relate the stopping power to the dielectric properties of a plasma medium [3]. The QCD analogue of this familiar problem has attracted some attention recently with the hope that the modification of jets in high-energy nucleus-nucleus collisions may be used as a probe of the quark-gluon plasma (QGP) produced by the collisions [4–7]. In his unpublished work, Bjorken [4] first estimated the energy loss of a high-energy parton (quark or gluon) prowling in the quark-gluon plasma due to elastic scattering with plasma constituents. This calculation of the energy-loss formula requires one to introduce an artificial cutoff parameter in the otherwise logarithmically divergent integral over the transferred momentum which arises due to the long-range nature of parton interactions in lowest-order QCD. As is well known, the infrared cutoff of the long-range Coulomb interaction in the ordinary plasma is caused by the dynamic screening which is calculable by the standard linear response theory [3]. This method was applied recently by Thoma and Gyulassy [8] to calculate the parton stopping power. A more thorough field-theoretical calculation of the stopping power including both the medium effect and the short-distance collisions was also presented by Braaten and Thoma [9].

Our purpose in writing this paper is twofold. We first discuss the mechanism of the energy deposition by a high-energy parton in the quark-gluon plasma in a pedagogical fashion in terms of the semiclassical kinetic theory and show how the energy lost by the parton will be distributed in the plasma. This question may be of special interest in the problem of the energy deposition by the minijets at collider energies [10]. It also provides us with intuitive physical insight about the plasma response to such an external probe. The second purpose is to extend this method to calculate the stopping power of a color dipole. This problem may be relevant for the distortion of heavy-quarkonium production by plasma formation [11].

The outline of the paper is the following. In Sec. II, we first derive the dielectric functions of the plasma which are necessary to calculate the energy loss of external partons based on semiclassical kinetic theory. We consider a baryon-free quark-gluon plasma at zero chemical potential which may be formed in the central rapidity region of ultrarelativistic nucleus-nucleus collisions [12] and treat it as an "Abelian plasma" in the sense that we ignore the non-Abelian features of the QCD interaction which may cause a certain modification in the transport equation [13]. As will be shown later, however, our method gives the same result for the dielectric function of the quark-gluon plasma as that calculated by the finite-temperature field theory in the lowest order of QCD coupling and in the high-temperature limit [14–17]. Use of this part of the dielectric functions is also supported by the recent perturbative QCD study at finite temperature based on the resummation technique [17].

In Sec. III, we discuss the stopping power for a single color-charged particle using the dielectric function obtained in Sec. II. This section has some overlap with previous studies [8,9]. Our energy-loss formula is simply a Lorentz force [8] caused by the electric field in the plasma medium and thus, in its original sense, should be used for the energy loss by soft-gluon exchange. However, as discussed in Ref. [9], it can be used for the total stopping power (within the 10% level) with an appropriate ultraviolet cutoff determined by the kinematic constraint. For a typical jet energy ($\sim$ 10 GeV), the resulting stopping power turns out to be 0.4–1.0 GeV/fm depending on the plasma parameters (strong-coupling constant, Debye mass). A new thing explored in this section is the pattern

*Present address.

of the energy distribution supplied by the external particle. We calculate the spatial distribution of the energy deposited per unit time per unit volume in the plasma from the first moment of the kinetic equation and examine how this pattern depends on the velocity of the external particle. Our result furnishes an intuitive way to look at the energy-deposition mechanism.

In Sec. IV, we calculate the stopping power of a color dipole ($c\bar{c}, b\bar{b}$) passing through the QGP, extending the method used in the foregoing section. Our main finding in this section can be summarized as follows. The energy loss for a color-neutral $Q\bar{Q}$ pair due to a relatively small momentum transfer ($\sim$less than inverse size of the pair) is about 1 order of magnitude smaller than the corresponding energy loss of a single color-charged particle, as is expected on the basis of "color transparency." However, an extremely high-energy $Q\bar{Q}$ pair whose size exceeds the inverse of the pair momentum can lose its energy by short-distance collisions with the plasma constituents. (Here short distance means smaller than the size of the dipole.) In this case the energy loss of the pair becomes the incoherent sum of the energy loss of each quark. Another interesting feature of the energy loss of the color dipole is its dependence on the orientation of the dipole with respect to the velocity: A longitudinally aligned dipole undergoes a larger stopping power than the transversely aligned case. We show how this can be understood intuitively by inspecting the spatial distribution of the energy supplied by the dipole. In Sec. V, we give a short summary of our findings.

II. DIELECTRIC PROPERTIES OF A RELATIVISTIC PLASMA IN THE KINETIC THEORY

In this section we summarize the kinetic theory description of the dielectric properties of a relativistic plasma which will be needed in our later discussion of the plasma stopping power. We begin with the microscopic form of Maxwell's equations which can be written in terms of the Fourier components of the fields as

$$\mathbf{k}\times\mathbf{e}(\omega,\mathbf{k})-\omega\mathbf{b}(\omega,\mathbf{k})=0 , \tag{2.1}$$

$$\mathbf{k}\times\mathbf{b}(\omega,\mathbf{k})+\omega\mathbf{e}(\omega,\mathbf{k})=-i[\mathbf{j}_{\rm ind}(\omega,\mathbf{k})+\mathbf{j}_{\rm ext}(\omega,\mathbf{k})] , \tag{2.2}$$

$$\mathbf{k}\cdot\mathbf{e}(\omega,\mathbf{k})=-i[\rho_{\rm ind}(\omega,\mathbf{k})+\rho_{\rm ext}(\omega,\mathbf{k})] , \tag{2.3}$$

$$\mathbf{k}\cdot\mathbf{b}(\omega,\mathbf{k})=0 , \tag{2.4}$$

where $\mathbf{e}(\omega,\mathbf{k})$ and $\mathbf{b}(\omega,\mathbf{k})$ are the Fourier components of microscopic electric and magnetic fields, respectively, and $\rho_{\rm ind}(\omega,\mathbf{k})$ and $\mathbf{j}_{\rm ind}(\omega,\mathbf{k})$ denote the Fourier components of the microscopic charge density and current density, respectively, induced in the plasma in the presence of the external charge density $\rho_{\rm ext}(\omega,\mathbf{k})$ and current density $\mathbf{j}_{\rm ext}(\omega,\mathbf{k})$. The microscopic-induced charge density and current contain a random fluctuation due to the microscopic fine structure of the plasma and this also gives rise to the fluctuations in the microscopic fields. The macroscopic Maxwell equations for a plasma are obtained from these equations by replacing fluctuating microscopic variables by smoothed macroscopic variables, taking the average over some semimicroscopic scale.

In the kinetic theory, the average charge density and current density induced in the plasma are given, respectively, by

$$\wp_{\rm ind}(t,\mathbf{r})\equiv\bar{\rho}_{\rm ind}(t,\mathbf{r}) = \sum_\sigma q_\sigma \int \frac{d^3p}{(2\pi)^3} f_\sigma(\mathbf{r},\mathbf{p};t) , \tag{2.5}$$

$$\mathbf{J}_{\rm ind}(t,\mathbf{r})\equiv\bar{\mathbf{j}}_{\rm ind}(t,\mathbf{r}) = \sum_\sigma q_\sigma \int \frac{d^3p}{(2\pi)^3} \mathbf{v}_p f_\sigma(\mathbf{r},\mathbf{p},t) , \tag{2.6}$$

where $\mathbf{v}_p=\mathbf{p}/\varepsilon_p$ is the velocity of plasma constituents with energy momentum $(\varepsilon_p,\mathbf{p})$ and $f_\sigma(\mathbf{r},\mathbf{p};t)$ is the single-particle distribution function of species σ (spin, color, flavor) in the single-particle phase space $(\mathbf{r},\mathbf{p})$ whose time evolution is determined by the Boltzmann-Vlasov equations

$$\frac{\partial f_\sigma}{\partial t}+\mathbf{v}_p\cdot\frac{\partial f_\sigma}{\partial \mathbf{r}}+q_\sigma(\mathbf{E}+\mathbf{v}_p\times\mathbf{B})\cdot\frac{\partial f_\sigma}{\partial \mathbf{p}}=\left[\frac{\partial f_\sigma}{\partial t}\right]_{\rm coll} , \tag{2.7}$$

where $\mathbf{E}$ and $\mathbf{B}$ are the macroscopic average electric and magnetic fields, respectively. The right-hand side of (2.7) is the collision term which contains the effects which arise due to the random fluctuations in microscopic quantities in the plasma [3]. We shall neglect these effects in the following derivation of the plasma stopping power formula. This approximation leads to the neglect of the dissipative effect as is usually accompanied by the friction force on the test charge [18].

The macroscopic Maxwell equations for the plasma can be written as

$$\mathbf{k}\times\mathbf{E}(\omega,\mathbf{k})-\omega\mathbf{B}(\omega,\mathbf{k})=0 , \tag{2.8}$$

$$\mathbf{k}\times\mathbf{B}(\omega,\mathbf{k})+\omega\mathbf{D}(\omega,\mathbf{k})=-i\mathbf{j}_{\rm ext}(\omega,\mathbf{k}) , \tag{2.9}$$

$$\mathbf{k}\cdot\mathbf{D}(\omega,\mathbf{k})=-i\rho_{\rm ext}(\omega,\mathbf{k}) , \tag{2.10}$$

$$\mathbf{k}\cdot\mathbf{B}(\omega,\mathbf{k})=0 , \tag{2.11}$$

where the displacement $\mathbf{D}(\omega,\mathbf{k})$ is defined, as usual, by

$$\mathbf{D}(\omega,\mathbf{k})=\mathbf{E}(\omega,\mathbf{k})+\mathbf{P}(\omega,\mathbf{k}) \tag{2.12}$$

with the polarization vector $\mathbf{P}(\omega,\mathbf{k})$ introduced by

$$-i\omega\mathbf{P}(\omega,\mathbf{k})=\mathbf{J}_{\rm ind}(\omega,\mathbf{k}) , \tag{2.13}$$

which also satisfies $i\mathbf{k}\cdot\mathbf{P}(\omega,\mathbf{k})=-\wp_{\rm ind}(\omega,\mathbf{k})$ due to the current conservation $\mathbf{k}\cdot\mathbf{J}_{\rm ind}(\omega,\mathbf{k})+\omega\wp_{\rm ind}(\omega,\mathbf{k})=0$. When there is a linear relation between the polarization vector and the average electric field (Ohm's law), we can write the constitutive relation

$$\mathbf{D}(\omega,\mathbf{k})=\boldsymbol{\epsilon}(\omega,\mathbf{k})\cdot\mathbf{E}(\omega,\mathbf{k}) , \tag{2.14}$$

which defines the dielectric permittivity tensor $\boldsymbol{\epsilon}(\omega,\mathbf{k})$ of the plasma. This tensor characterizes the dielectric properties of the plasma medium. One of the most important characteristics of the plasma is that $\boldsymbol{\epsilon}(\omega,\mathbf{k})$ has both spa-

tial and time dispersion and it is a matrix. For the isotropic medium, the dielectric tensor can be decomposed in the rest frame of the plasma into two components:

$$\epsilon_{ij}(\omega,\mathbf{k})=\epsilon_L(\omega,k)\frac{k_i k_j}{k^2}+\epsilon_T(\omega,k)\left[\delta_{ij}-\frac{k_i k_j}{k^2}\right], \quad (2.15)$$

where the scalar functions ϵ_L and ϵ_T are the longitudinal and transverse dielectric functions, respectively [19].

The normal modes in the plasma can be found by solving Eq. (2.8) for **B** and inserting it into Eq. (2.9). This gives

$$\mathbf{\Delta}(\omega,\mathbf{k})\cdot\mathbf{E}(\omega,\mathbf{k})=-\frac{i}{\omega}\mathbf{j}_{\rm ext}(\omega,\mathbf{k}), \quad (2.16)$$

where the matrix $\mathbf{\Delta}$ is defined by

$$\Delta_{ij}(\omega,\mathbf{k})\equiv\epsilon_{ij}(\omega,\mathbf{k})-\frac{k^2}{\omega^2}\left[\delta_{ij}-\frac{k_i k_j}{k^2}\right]. \quad (2.17)$$

The dispersion relations for the normal modes are determined by the condition that Eq. (2.12) has a nontrivial solution with $\mathbf{j}_{\rm ext}=0$. This condition reads

$$\det\mathbf{\Delta}(\omega,\mathbf{k})=0. \quad (2.18)$$

For the isotropic medium, this condition can be written in terms of the longitudinal and transverse dielectric functions ϵ_L and ϵ_T:

$$\epsilon_L(\omega,\mathbf{k})=0, \quad \epsilon_T(\omega,\mathbf{k})=\frac{k^2}{\omega^2}. \quad (2.19)$$

The functional form of the plasma dielectric functions is determined by calculating the induced current which appears in the Maxwell equations in the linear response approximation with respect to the field. Suppose that the plasma is in a stationary homogeneous state at $t=-\infty$ with the distribution function $f_\sigma(\mathbf{r},\mathbf{p};-\infty)=f^0_\sigma(\mathbf{p})$. Any distribution function which is independent of the spatial coordinate is a solution of the Boltzmann-Vlasov equations (2.7) in the absence of the collision term because **E** and **B** vanishes identically due to the overall charge neutrality. The electric- and magnetic-field disturbance is then turned on adiabatically as $(\eta\to+0)$

$$\mathbf{E}(\mathbf{r},t)=\delta\mathbf{E}(\omega,\mathbf{k})\exp[-i(\omega t-\mathbf{k}\cdot\mathbf{r})+\eta t],$$

$$\mathbf{B}(\mathbf{r},t)=\frac{1}{\omega}\mathbf{k}\times\delta\mathbf{E}(\omega,\mathbf{k})\exp[-i(\omega t-\mathbf{k}\cdot\mathbf{r})+\eta t],$$

in accordance with Eqs. (2.8) and (2.11). In response to these perturbations, the distribution function receives a small disturbance:

$$f_\sigma(r,\mathbf{p};t)=f^0_\sigma(\mathbf{p})+\delta f_\sigma(\mathbf{p};\omega,\mathbf{k})\times\exp[-i(\omega t-\mathbf{k}\cdot\mathbf{r})+\eta t]. \quad (2.20)$$

Substituting the above three equations into the collisionless Boltzmann-Vlasov equation, (2.8), in the absence of the collision term, we find

$$i(\omega+i\eta-\mathbf{v}_p\cdot\mathbf{k})\delta f_\sigma(\mathbf{p};\omega,\mathbf{k})=q_\sigma\frac{\partial f^0_\sigma(\mathbf{p})}{\partial p_i}\left[\left[1-\frac{\mathbf{k}\cdot\mathbf{v}_p}{\omega}\right]\delta_{ij}+\frac{k_i v_{p,j}}{\omega}\right]\delta E_j. \quad (2.21)$$

We solve (2.21) for δf_σ, and insert it into (2.20). The substitution of the result into (2.6) establishes the linear relationship between the induced current and the field (Ohm's law)

$$\delta J_i(\omega,\mathbf{k})=\sigma_{ij}(\omega,\mathbf{k})\delta E_j(\omega,\mathbf{k}) \quad (2.22)$$

with the conductivity tensor given by

$$\sigma_{ij}(\omega,\mathbf{k})=-i\sum_\sigma q_\sigma^2\int\frac{d^3p}{(2\pi)^3}\frac{p_i}{\varepsilon_p}\frac{1}{\omega-\mathbf{v}_p\cdot\mathbf{k}+i\eta}\times\left[\left[1-\frac{\mathbf{k}\cdot\mathbf{v}_p}{\omega}\right]\frac{\partial f^0_\sigma(\mathbf{p})}{\partial p_j}+\mathbf{k}\cdot\frac{\partial f^0_\sigma(\mathbf{p})}{\partial\mathbf{p}}\frac{v_{p,j}}{\omega}\right], \quad (2.23)$$

from which we can determine the form of the dielectric tensor by the relation

$$\epsilon_{ij}(\omega,\mathbf{k})=\delta_{ij}+\frac{i}{\omega}\sigma_{ij}(\omega,\mathbf{k}), \quad (2.24)$$

which follows from (2.12) and (2.13). If we take the Bose-Einstein or Fermi-Dirac distribution $f^0_\sigma(\mathbf{p})=1/(e^{\beta\varepsilon_p}\pm1)$ for the undisturbed stationary distribution and let all the plasma constituents be massless ($\varepsilon_p=p$), then we obtain the well-known result [20]

$$\epsilon_L(\omega,k)=1+\frac{m_D^2}{k^2}\left[1+\frac{\omega}{2k}\ln\left|\frac{\omega-k}{\omega+k}\right|+\frac{i\pi\omega}{2k}\theta(k-|\omega|)\right], \quad (2.25)$$

$$\epsilon_T(\omega,k)=1+\frac{m_D^2}{\omega k}\left[-\frac{\omega}{2k}+\frac{1}{4}\left[1-\frac{\omega^2}{k^2}\right]\ln\left|\frac{\omega-k}{\omega+k}\right|+\frac{i\pi}{4}\left[1-\frac{\omega^2}{k^2}\right]\theta(k-|\omega|)\right], \quad (2.26)$$

where m_D is the Debye screening mass given by

$$m_D^2=\sum_\sigma c_\sigma q_\sigma^2 T^2, \quad (2.27)$$

with $c_\sigma=\frac{1}{12}$ ($\frac{1}{6}$) for a fermion (boson). For the case of electromagnetic plasma consisting of e^+ and e^-,

$$m_D^2=(e^2/12)T^2\times2\times2\ (\text{spin and } e^+e^-)=e^2T^2/3.$$

The above formulas for ϵ_L and ϵ_T are the same as the leading-order gauge-invariant part of the high-temperature expansion of the perturbative result (i.e., $T\gg\omega,k$) [14–17], if we identify the sum over "charge q_σ" in Eq. (2.27) as

$$\sum_{\text{quark}} q_\sigma^2 \to 4N_f \left[\frac{g}{2}\right]^2 \mathrm{Tr}(\lambda^a\lambda^b)=2N_f g^2\delta_{ab},$$

$$\sum_{\text{gluon}} q_\sigma^2 \to 2g^2 f_{acd}f_{bcd}=6g^2\delta_{ab} ,$$

and thus $m_D^2=g^2T^2(1+N_f/6)$ [11]. Use of Eqs. (2.25) and (2.26) is also supported by recent perturbative QCD analysis of finite-temperature gluon polarization based on the resummation technique [17].

III. ENERGY LOSS OF A SINGLE PARTON

After these preparations it is now easy to derive the stopping power for an external parton passing through a quark-gluon plasma. Suppose a parton with charge Q is moving in the plasma with a fixed velocity $\mathbf{v}$. The external current density created by the parton charge is

$$\mathbf{j}_{\text{ext}}(\omega,\mathbf{k})=2\pi Q\mathbf{v}\delta(\omega-\mathbf{v}\cdot\mathbf{k}) . \tag{3.1}$$

Then Eq. (2.16) gives the electric field as

$$\begin{aligned}\mathbf{E}(\omega,\mathbf{k})&=-\frac{i}{\omega}\boldsymbol{\Delta}^{-1}(\omega,\mathbf{k})\cdot\mathbf{j}_{\text{ext}}(\omega,\mathbf{k})\\&=-i2\pi Q\left[\frac{\mathbf{k}}{k^2\epsilon_L(\omega,k)}+\frac{\omega(\mathbf{v}-\mathbf{k}\omega/k^2)}{\omega^2\epsilon_T(\omega,k)-k^2}\right]\\&\quad\times\delta(\omega-\mathbf{v}\cdot\mathbf{k}) .\end{aligned} \tag{3.2}$$

The stopping power of the plasma, namely, the energy loss of the parton per unit length, is simply the Lorentz force exerted on the parton charge in the direction opposite to the parton's motion by the electric field created at the position where the parton resides [12]:

$$\begin{aligned}-\frac{dE}{dx}&=-Q\frac{\mathbf{v}}{v}\cdot\mathbf{E}(\mathbf{r}=\mathbf{v}t,t)\\&=-\frac{Q}{(2\pi)^4}\int d^3k\,d\omega\frac{\mathbf{v}}{v}\cdot\mathbf{E}(\omega,k)e^{-i\omega t+i\mathbf{v}\cdot\mathbf{k}t} .\end{aligned} \tag{3.3}$$

Inserting (3.2) into (3.3) and noting that the real part of the dielectric functions $\epsilon_L(\omega,k)$ and $\epsilon_T(\omega,k)$ is an even function of ω while the imaginary part is an odd function so that only the imaginary part of ϵ_L^{-1} and $(\omega^2\epsilon_T-k^2)^{-1}$ survives the integration, we obtain the following expression for the stopping power:

$$\frac{-dE}{dx}=-\frac{C_Q\alpha_s}{2\pi^2 v}\int d^3k\,d\omega\,\omega\left[\frac{1}{k^2}\mathrm{Im}\frac{1}{\epsilon_L(\omega,k)}+\left[v^2-\frac{\omega^2}{k^2}\right]\mathrm{Im}\frac{1}{\omega^2\epsilon_T(\omega,k)-k^2}\right]\delta(\omega-\mathbf{v}\cdot\mathbf{k}) , \tag{3.4}$$

where we have replaced $Q^2/4\pi$ by $C_Q\alpha_s$ with the strong-coupling constant $\alpha_s=g^2/4\pi$ and the Casimir invariant for an SU(3) charge Q; $C_Q=\frac{4}{3}$ (3) for a quark (gluon). This formula is the relativistic extension of the well-known formula for the plasma stopping power [3].

The above formula for the plasma stopping power contains both the energy loss due to the collective plasma response and that due to the scatterings with individual plasma constituents. One can see this by dividing the integral over the transferred momentum k into two distinct regions: short wavelength ($k_0<k$) and long wavelength ($k<k_0$), where k_0 is a momentum of the order of the Debye screening mass m_D. In a short-wavelength region, it is a good approximation to set simply $|\epsilon_L|=|\epsilon_T|=1$ so that the contribution to the stopping power from this part of the integral is

$$\left[-\frac{dE}{dx}\right]_{k>k_0}\simeq\frac{C_Q\alpha_s m_D^2}{4\pi v}\int_{k_0<k}\frac{d^3k}{k}\int d\omega\,\omega^2\left[\frac{1}{k^4}+\frac{1}{2}\left[1-\frac{\omega^2}{k^2}\right]\left[v^2-\frac{\omega^2}{k^2}\right]\frac{1}{(\omega^2-k^2)^2}\right]\delta(\omega-\mathbf{v}\cdot\mathbf{k}) . \tag{3.5}$$

Noting that $m_D^2\sim\alpha_s T^2$, it is now evident that this is nothing but the energy loss of the parton due to the scattering with individual plasma constituents at short distances ($r<1/m_D$). The first term in the parentheses corresponds to the Coulomb scattering and the second to the magnetic scattering. The above phase-space integration can be performed easily and we find

$$\left[-\frac{dE}{dx}\right]_{k>k_0}=\frac{C_Q\alpha_s m_D^2}{2}\frac{1}{v^2}\left[v+\frac{1-v^2}{2}\ln\left[\frac{1-v}{1+v}\right]\right]\times\ln(k_{\max}/k_0) , \tag{3.6}$$

where we have introduced a cutoff $k_{\max}$ in the otherwise logarithmically divergent integral over k. This logarithmic ultraviolet divergence has arisen due to the assumption implicit in our derivation that the external parton moves on the straight-line trajectory without recoil and that the motion of the plasma constituents is "averaged" as a form of dielectric tensor of the plasma; this approximation fails at the very short distances comparable to the mean interparticle distance in the plasma due to the deflection of the parton by the scattering with individual plasma constituents when the transferred momentum is comparable to the momentum of the parton and/or plasma constituents.

A more thorough discussion about the energy loss including both medium effects and the short-distance collision was given by Braaten and Thoma [9] using the microscopic Feynman-diagram calculation. There it is shown that we can use Eq. (3.4) as a total stopping power with an appropriate cutoff for the momentum integral,

$k_{\max}$, except for a tiny correction factor. The collision kinematics, which is relevant to determine the cutoff $k_{\max}$, is discussed in the Appendix: For a massless parton and a very fast massive parton ($v \to 1$) with energy E, $E \gg T, M^2/T$ (M is the mass of the parton and T is the plasmon temperature), the maximum momentum transfer is $k_{\max} \sim E$. For a massive parton with moderate energy, $M \ll E \ll M^2/T$, $k_{\max} \sim 2q/(1-v) \sim 2T/(1-v)$, where q is the energy of the plasma constituent (its precise form is not as important since the divergence is logarithmic).

The contribution from the long-distance part of the interaction,

$$\left[-\frac{dE}{dx}\right]_{k<k_0} = -\frac{C_Q \alpha_s}{\pi v^2}\int_0^{k_0}\frac{dk}{k}\int_{-vk}^{vk} d\omega\,\omega\,\mathrm{Im}\left[\frac{1}{\epsilon_L(\omega,k)} + \frac{v^2k^2-\omega^2}{\omega^2\epsilon_T(\omega,k)-k^2}\right], \tag{3.7}$$

includes the effect of the collective plasma response through the dielectric functions so that the integral in the infrared region $k \to m_D$ becomes finite due to the plasma screening. We note that this long-range part of the plasma stopping power depends only on the velocity of the partons, but not on its momentum explicitly. For the comparative study with the dipole stopping power in the next section, we plot in Fig. 1 the numerical values of the long-distance part $(-dE/dx)_{k<k_0}$ for two values of k_0, m_D, and $2m_D$, with $m_D = 600$ MeV and $\alpha_s = 0.3$ (approximately equal to the data from recent results of lattice QCD calculation [21,22]). If we identify the Debye mass as the perturbative one as $m_D = gT\sqrt{1+N_f/6}$, these values correspond to $T = 270$ MeV with $N_f = 2$. In Fig. 1 we plotted the longitudinal part [the first term of Eq. (3.7)] and the transverse component [the second term of Eq. (3.7)] separately. We can see from the figure that the stopping power is dominated by the longitudinal component.

With the same values for the parameters m_D and α_s we find, for the short-distance part (3.6),

$$\left[-\frac{dE}{dx}\right]_{k>k_0} = 0.36\frac{1}{v^2}\left[v + \frac{1-v^2}{2}\ln\left[\frac{1-v}{1+v}\right]\right] \times \ln(k_{\max}/k_0)\ \mathrm{GeV/fm}\ , \tag{3.8}$$

which gives $(-dE/dx)_{k>k_0} = 1.0(0.76)$ GeV/fm if we take $k_{\max} = E = 10$ GeV, $k_0 = m_D = 600$ MeV ($2m_D = 1.2$ GeV), and $v = 1$, which is much greater than the long-distance part of the stopping power shown at Fig. 1. In short, for a massless parton and a very fast massive parton with the energy $E \gg T, M^2/T$, Eq. (3.6) with $k_0 = m_D$ and $k_{\max} = E$ is a good approximation for the total stopping power, while for $M \ll E \ll M^2/T$, Eq. (3.4) should be used with $k_{\max} = 2T/(1-v)$. We note that these numerical values are very sensitive to the choice of the screening mass m_D^2 and, if we take $m_D = 400$ or 800 MeV in place of 600 MeV, we find $(-dE/dx)_{k>k_0} = 0.44$ or 1.7 GeV/fm with $k_0 = m_D$. We note in passing a stopping power with the plasma parameter obtained in a quenched lattice calculation by Gao [22]: It gives $\alpha_s \simeq 0.12$ and $m_D \simeq 4.5T_c \simeq 700$–$900$ MeV at $T \simeq 1.5T_c \simeq 250$–$300$ MeV, which results in $(-dE/dx) \simeq 0.54$–0.9 GeV/fm for the above case.

At this point one may wish to recall the nonrelativistic formula for the collisional energy loss of a charged particle in a dense medium, whose velocity dependence takes the form of $(1/v^2)(\ln v + \text{const})$ at a small velocity. This behavior appears in ordinary plasma physics because one can replace the boundary of the ω integration by $\int_{-\infty}^{\infty} d\omega$ due to the condition that the velocity of the particle is much larger than the thermal velocity of the plasma constituents $v_{\mathrm{th}} = (T/m)^{1/2}$ since their motion is nonrelativistic. Then one can employ the sum rule to carry out the integration over the transferred energy ω [3]. In our case this replacement is not allowed since our plasma consists of massless quarks and gluons and they are all moving at the light velocity and therefore the region of ω integration is limited to the spacelike region ($|\omega| < k$) even at maximum velocity $v = 1$ by scattering kinematics. The resultant ω integral becomes strongly velocity dependent and thus alters the v dependence of the stopping power from the well-known nonrelativistic result. The change of the velocity dependence is thus caused by the

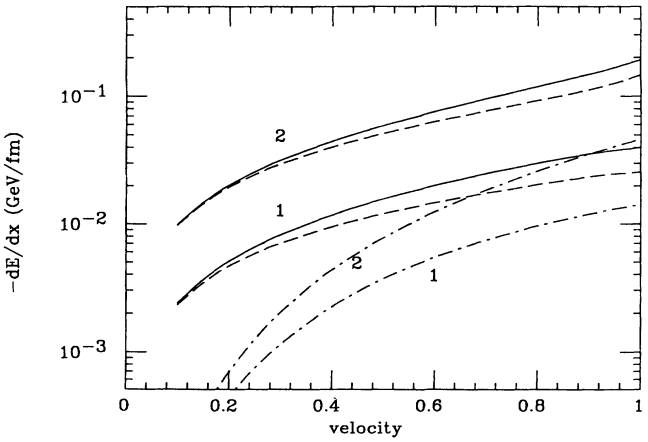

FIG. 1. Stopping power for a quark due to the long-range effects using two cutoffs: (1) m_D, (2) $2m_D$. Dashed lines are the longitudinal part, dash-dotted lines are the transverse part, and solid lines are the sum of these two.

breakdown of the nonrelativistic sum rule in the relativistic regime. (A similar effect is known in the Coulomb sum rule [23].)

The same kinematic constraint leads to another important difference of the mechanism of energy loss in relativistic plasmas from that in nonrelativistic plasmas; namely, the absence of the Cherenkov emission of the collective plasmons. In the nonrelativistic plasma the energy loss by the long-distance part of the interaction is dominated by the pole of $1/\epsilon_L(\omega,k)$, which corresponds to the excitation of the collective modes since the plasmon dispersion relation is given by $\epsilon_L(\omega,k)=0$. The same thing would occur if the integral in (3.7) goes through the pole of the integrand; this, however, does not happen in our case since the plasmon dispersion relation for the ultrarelativistic (massless) plasma is always timelike while the energy and the momentum provided by the external probe is always spacelike.

Further insight on the energy-loss mechanism may be obtained by studying the spatial distribution of the energy deposited by the parton in the plasma. For this purpose, we first calculate the divergence of the kinetic energy-momentum tensor of the plasma,

$$T^{\mu\nu}(x)=\sum_{\sigma}\int\frac{d^3p}{(2\pi)^3}\frac{p^\mu p^\nu}{\varepsilon_p}f_\sigma(\mathbf{r},\mathbf{p};t)\ , \tag{3.9}$$

from the collisionless Boltzmann-Vlasov equation (2.7). The result can be written in a concise form as

$$\partial_\mu T^{\mu\nu}(x)=F^\nu{}_\mu(x)\bar{j}^\mu_{\rm ind}(x)\ . \tag{3.10}$$

The time component ($\nu=0$) of this equation simply means that the rate of the energy absorption by unit volume of plasma is given by the work done by the electric field on the charged plasma constituents per unit volume,

$$\frac{d^4W}{dt\,d^3r}=\mathbf{E}(x)\cdot\mathbf{J}_{\rm ind}(x)\ , \tag{3.11}$$

while the spatial components express the rate of the momentum absorption per unit volume of plasma.

Let us first check with these relations that the energy lost by the external test charge is equal to the increase in the kinetic energy of the plasma constituents. The total energy supplied to the plasma from the parton per unit time is

$$\begin{aligned}\frac{dW}{dt}&=\int d^3r\,\mathbf{E}(x)\cdot\mathbf{J}_{\rm ind}(x)\\&=\frac{1}{(2\pi)^5}\int d\omega\int d\omega'\int d^3k\,\mathbf{E}(\omega,\mathbf{k})\\&\qquad\times\mathbf{J}_{\rm ind}(\omega',-\mathbf{k})e^{i(\omega+\omega')t}\ .\end{aligned} \tag{3.12}$$

Substituting the Fourier components of the induced current

$$J_{{\rm ind},i}(\omega,\mathbf{k})=-i\omega[\epsilon_{ij}(\omega,\mathbf{k})-\delta_{ij}]E_j(\omega,\mathbf{k})$$

into (3.12), and then using (3.2) for the electric field,

$$\begin{aligned}\frac{dW}{dt}=-\frac{C_F\alpha_s i}{2\pi^2}\int d^3k\,d\omega\,\omega\Bigg[&\frac{1}{k^2\epsilon_L(\omega,k)}+\frac{v^2-\omega^2/k^2}{\omega^2\epsilon_T(\omega,k)-k^2}-\frac{1}{k^2\epsilon_L(\omega,k)\epsilon_L(-\omega,k)}\\&-\frac{(v^2-\omega^2/k^2)(\omega^2-k^2)}{[\omega^2\epsilon_T(\omega,k)-k^2][\omega^2\epsilon_T(-\omega,k)-k^2]}\Bigg]\delta(\omega-\mathbf{v}\cdot\mathbf{k})\ .\end{aligned} \tag{3.13}$$

The last two terms in the large parentheses, as well as the real part of the first two terms, are even functions of ω so that they vanish upon integration over ω. Therefore, we obtain

$$\frac{dW}{dt}=-\frac{C_F\alpha_s}{2\pi^2}\int d^3k\,d\omega\,\omega\left[\frac{1}{k^2}\mathrm{Im}\frac{1}{\epsilon_L(\omega,k)}+\left[v^2-\frac{\omega^2}{k^2}\right]\mathrm{Im}\frac{1}{\omega^2\epsilon_T(\omega,k)-k^2}\right]\delta(\omega-\mathbf{v}\cdot\mathbf{k})\ . \tag{3.14}$$

Comparing with the formula for the plasma stopping power (3.4), we find

$$\frac{dW}{dt}=-v\frac{dE}{dx}\ , \tag{3.15}$$

which implies that the total energy received by the plasma constituents is indeed equal to the energy loss per unit time of the test charge.

We show in Fig. 2 the contour plots of several snapshots of $d^4W/dt\,d^3(x)$ in the rest frame of the plasma. In these graphs the test parton resides at the origin of the coordinate and is moving in the positive z direction with four different velocities: $v=0.3$, 0.6, 0.9, and 0.99. We plotted the contours only at relatively large distances from the parton [$r\geq 1/(2m_D)$] where the collective plasma response is more prominent. It is seen that, at relatively small parton velocities, the plasma gains energy in the forward hemisphere but loses energy in the backward hemisphere and, as the velocity increases, the region where $d^4W/dt\,d^3r$ becomes negative disappears. The appearance of the negative-energy region can be understood as a "pushing" effect of the plasma constituents in the backward hemisphere. In fact, in our relativistic plasma, all the plasma constituents are moving around isotropically at light velocity. When the longitudinal velocity of the plasma constituents in the backward hemisphere is

large enough in the positive z direction compared with the velocity of the external parton, they can efficiently transfer positive energy to the parton by the collision, and hence negative-energy deposition. All the other plasma constituents get energy from the incoming parton. Therefore, as the velocity of the external parton increases, the negative-energy region shrinks, and at the same time the transverse component of the electric field gets stronger by a factor $1/\sqrt{1-v^2}$ due to the Lorentz contraction and thus the energy is distributed strongly in the transverse direction. [See Figs. 2(c) and 2(d).] The pattern of the energy deposition shown in Fig. 2 can also be understood by considering the direction of $\mathbf{E}$ and $\mathbf{J}_{\rm ind}$. The electric field emanates from the external parton with some Lorentz contraction depending on the partons' velocity. Because of the presence of the incoming parton, the plasma constituents in front of the parton are "pushed away" once from the parton's position, then go around and come back to the original place from the back side. Correspondingly, the induced current $\mathbf{J}_{\rm ind}$ draws similar curves. Therefore, $\mathbf{E}\cdot\mathbf{J}_{\rm ind}$ exhibits the pattern shown in Fig. 2.

We note that this process of energy deposition in the plasma by a high-energy parton is *adiabatic;* that is, there is no increase of entropy associated with the energy transfer. This can be proved directly by calculating the divergence of the entropy current as defined by

$$s^{\mu}(x)=-\sum_{\sigma}\int\frac{d^3p}{(2\pi)^3}\frac{p^{\mu}}{\varepsilon_p}[f_{\sigma}\ln f_{\sigma}\mp(1\pm f_{\sigma})\ln(1\pm f_{\sigma})]\ . \tag{3.16}$$

Using the Boltzmann-Vlasov equation (2.7) one can show

$$\partial_{\mu}s^{\mu}(x)=\sum_{\sigma}q_{\sigma}\int\frac{d^3p}{(2\pi)^3}\left[[\mathbf{E}(x)+\mathbf{v}_p\times\mathbf{B}(x)]\cdot\frac{\partial f_{\sigma}}{\partial\mathbf{p}}-\left[\frac{\partial f_{\sigma}}{\partial t}\right]_{\rm coll}\right]\ln\left[\frac{f_{\sigma}}{1\pm f_{\sigma}}\right], \tag{3.17}$$

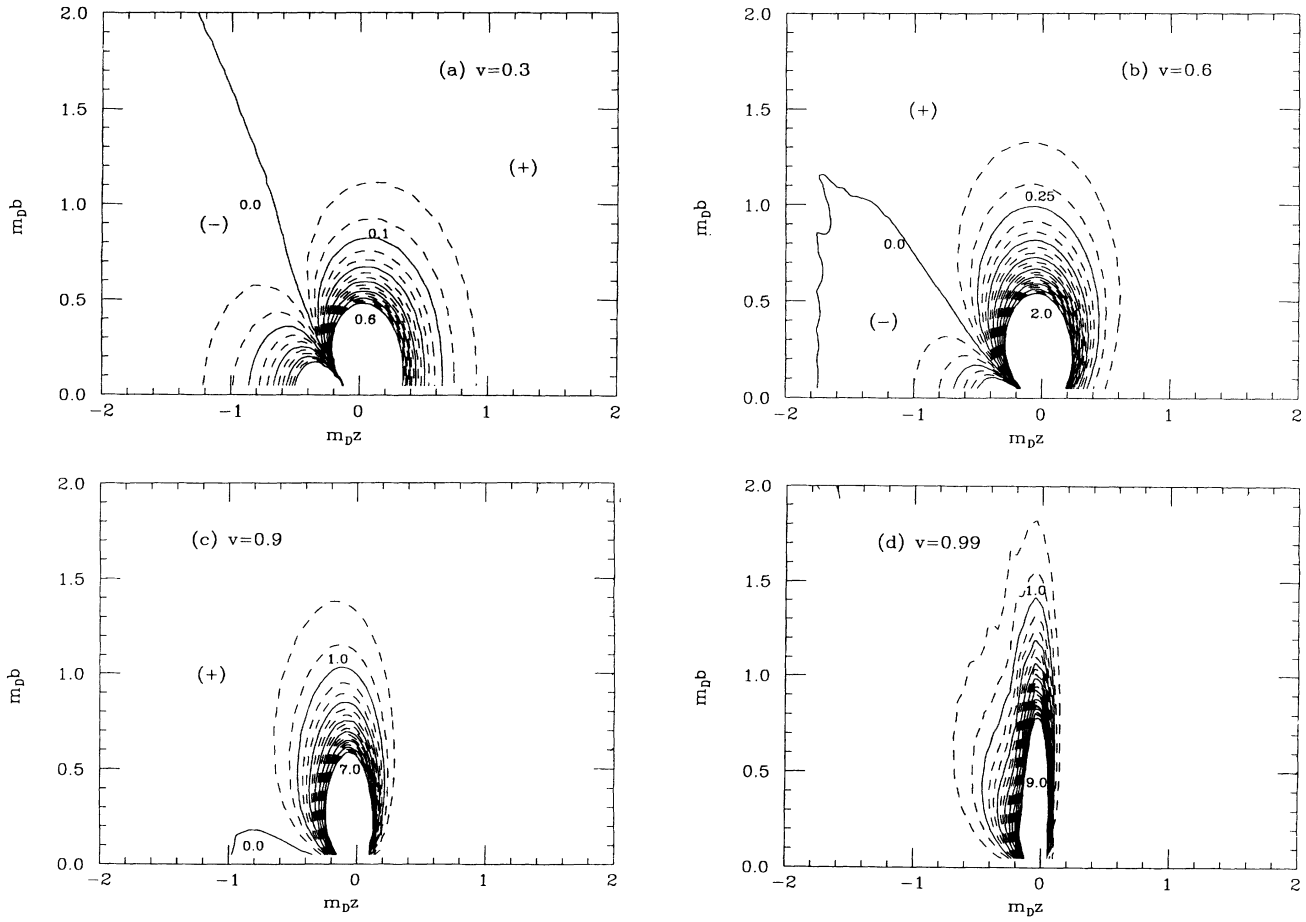

FIG. 2. Contour plots of the distribution of the energy supplied to plasma constituents by an external parton per unit time for four velocities of the parton: (a) $v=0.3$, (b) $v=0.6$, (c) $v=0.9$, (d) $v=0.99$. The external parton is at the origin of each figure and is moving into the positive z direction. The system has an azimuthal symmetry with respect to the z axis and the distribution is shown as a function of z and the collision parameter b. The lengths are shown in units of Debye mass m_D. The numbers attached to the contours indicate the energies in units of GeV/fm^3.

where the first term in the large square brackets can be converted to a vanishing surface term by using

$$\frac{\partial f_\sigma}{\partial \mathbf{p}} \ln\left[\frac{f_\sigma}{1\pm f_\sigma}\right] = \frac{\partial}{\partial \mathbf{p}}[f_\sigma \ln f_\sigma \mp (1\pm f_\sigma)\ln(1\pm f_\sigma)] \tag{3.18}$$

and $\mathbf{v}_p = \partial\varepsilon_p/\partial\mathbf{p}$. The divergence of the entropy current therefore indeed vanishes in the absence of a collision term. The mechanism of the energy deposition by the external test charge is essentially the same as that of the Landau damping of the collective plasma oscillation which occurs also in the absence of the collision term.

IV. ENERGY LOSS OF A COLOR DIPOLE

The foregoing analysis of the plasma stopping power for a single parton may be extended directly to a pair of partons with charges Q_1 and Q_2 moving together in the plasma with the same velocity v at a fixed separation r_0. The Fourier components of the external current generated by the pairs is given by

$$\begin{aligned}\mathbf{j}_{\rm ext}^{(\rm pair)}(\omega,\mathbf{k}) &= \int dt\, d^3r\, e^{i\omega t - i\mathbf{k}\cdot\mathbf{r}}\left[Q_1\mathbf{v}\delta^3\left(\mathbf{r}-\frac{\mathbf{r}_0}{2}-\mathbf{v}t\right)+Q_2\mathbf{v}\delta^3\left(\mathbf{r}+\frac{\mathbf{r}_0}{2}-\mathbf{v}t\right)\right] \\ &= 2\pi\mathbf{v}\delta(\omega-\mathbf{v}\cdot\mathbf{k})\left[Q_1\exp\left[-\frac{i}{2}\mathbf{k}\cdot\mathbf{r}_0\right]+Q_2\exp\left[\frac{i}{2}\mathbf{k}\cdot\mathbf{r}_0\right]\right] .\end{aligned} \tag{4.1}$$

For small $k(\ll 1/r_0)$ the exponentials can be expanded as a power series of kr_0, yielding multipole expansion whose leading terms are given by

$$\mathbf{j}_{\rm ext}^{(\rm pair)}(\omega,\mathbf{k}) = 2\pi\mathbf{v}\delta(\omega-\mathbf{v}\cdot\mathbf{k})\left[Q-\frac{i}{2}\mathbf{d}\cdot\mathbf{k}-\frac{Q}{8}(\mathbf{k}\cdot\mathbf{r}_0)^2+\cdots\right], \tag{4.2}$$

where the first term is the current produced by the point test charge (monopole) equivalent to the net charge on the pair $Q=Q_1+Q_2$ and the second term is the current by the motion of the dipole moment

$$\mathbf{d}=(Q_1-Q_2)\mathbf{r}_0 . \tag{4.3}$$

For a neutral pair the monopole term vanishes and the dipole term gives the leading contribution. The third term which contains the quadrupole current and a correction to the monopole current due to the finite-size effect will also vanish for a neutral pair.

In the linear response approximation, the electric field induced by this external current in the plasma is just the superposition of two fields which would be generated by each component of the pair in the absence of the other, and therefore the Fourier components of the electric field are

$$\begin{aligned}\mathbf{E}^{(\rm pair)}(\omega,\mathbf{k}) &= -\frac{i}{\omega}\boldsymbol{\Delta}^{-1}(\omega,\mathbf{k})\cdot\mathbf{j}_{\rm ext}^{(\rm pair)}(\omega,\mathbf{k}) \\ &= -i2\pi\left[\frac{\mathbf{k}}{k^2\epsilon_L(\omega,k)}+\omega\left[\mathbf{v}-\frac{\mathbf{k}\omega}{k^2}\right]\frac{1}{\omega^2\epsilon_T(\omega,k)-k^2}\right]\left[Q-\frac{i}{2}\mathbf{k}\cdot\mathbf{d}-\frac{Q}{8}(\mathbf{k}\cdot\mathbf{r}_0)^2+\cdots\right]\delta(\omega-\mathbf{v}\cdot\mathbf{k}) .\end{aligned} \tag{4.4}$$

The net force acting on the pair is given in terms of the field strength at the locations of the charges,

$$\begin{aligned}\mathbf{F}^{(\rm pair)} &= -Q_1\mathbf{E}^{(\rm pair)}\left[\frac{\mathbf{r}_0}{2}+\mathbf{v}t,t\right]-Q_2\mathbf{E}^{(\rm pair)}\left[-\frac{\mathbf{r}_0}{2}+\mathbf{v}t,t\right] \\ &= -Q\mathbf{E}^{(\rm pair)}(\mathbf{v}t,t)-\tfrac{1}{2}\mathbf{d}\cdot\left[\frac{\partial}{\partial\mathbf{r}}\mathbf{E}^{(\rm pair)}(\mathbf{r},t)\right]_{\mathbf{r}=\mathbf{v}t}-\frac{Q}{8}r_{0i}r_{0j}\left[\frac{\partial^2}{\partial r_i\partial r_j}\mathbf{E}^{(\rm pair)}(\mathbf{r},t)\right]_{\mathbf{r}=\mathbf{v}t}-\cdots ,\end{aligned} \tag{4.5}$$

which can be written in terms of the Fourier components of the field as

$$\mathbf{F}^{(\rm pair)} = -\frac{1}{(2\pi)^4}\int d^3k\, d\omega\left[Q+\frac{i}{2}\mathbf{k}\cdot\mathbf{d}-\frac{Q}{8}(\mathbf{k}\cdot\mathbf{r}_0)^2+\cdots\right]\mathbf{E}^{(\rm pair)}(\omega,\mathbf{k}) . \tag{4.6}$$

Substituting (4.4) into (4.6) we find

$$\mathbf{F}^{(\rm pair)} = \frac{i}{(2\pi)^3}\int d^3k\, d\omega\left[\frac{\mathbf{k}}{k^2\epsilon_L(\omega,k)}+\frac{\omega(\mathbf{v}-\omega\mathbf{k}/k^2)}{\omega^2\epsilon_T(\omega,k)-k^2}\right]\left[Q^2+\tfrac{1}{4}(\mathbf{k}\cdot\mathbf{d})^2-\frac{Q^2}{4}(\mathbf{k}\cdot\mathbf{r}_0)^2+\cdots\right]\delta(\omega-\mathbf{v}\cdot\mathbf{k}) . \tag{4.7}$$

It is not difficult to see from this expression that the direction of the force acting on the pair is always parallel to the

direction of the motion of the pair. (This is so because $\mathbf{v}$ is the only vector which can appear in the positions of the vector $\mathbf{k}$ after the integration over $\mathbf{k}$ and ω.) The stopping power on the pair is therefore given by

$$\left[-\frac{dE}{dx}\right]_{\text{pair}}=-\frac{1}{(2\pi)^3 v}\int d^3k\, d\omega\,\omega\,\text{Im}\left[\frac{1}{k^2\epsilon_L(\omega,k)}+\frac{v^2-\omega^2/k^2}{\omega^2\epsilon_T(\omega,k)-k^2}\right]\left[Q^2+\tfrac{1}{4}(\mathbf{k}\cdot\mathbf{d})^2-\frac{Q^2}{4}(\mathbf{k}\cdot\mathbf{r}_0)^2+\cdots\right]\delta(\omega-\mathbf{v}\cdot\mathbf{k})\,, \tag{4.8}$$

where we have again used the fact that the real and imaginary parts of $\epsilon_L(\omega,k)$ and $\epsilon_T(\omega,k)$ are, respectively, even and odd functions of ω so that only the imaginary part of the term in large parentheses survives the integration over ω.

This result may be transcribed for the case of non-Abelian charges through the following replacement: $Q^2=C_Q g^2$ and $(Q_1-Q_2)^2=2(Q_1^2+Q_2^2)-Q^2=C_d g^2$ with $C_d=4C_f-C_Q$, where C_Q is the Casimir invariant for the SU(3) representation of the net (non-Abelian) charge Q on the pair. For a color-octet pair ($C_Q=3$, $C_d=\frac{7}{3}$), the leading monopole term gives the same result as we obtained in the previous section for a single octet parton (gluon) and the corrections due to the finite extension of the system are negative. (Note that the incoherent sum of the contributions from two color-triplet charges would give $\frac{8}{3}$ in place of 3 for C_Q.) On the other hand, for a color-singlet pair, $C_Q=0$ so that the leading contribution is the dipole term

$$\left[-\frac{dE}{dx}\right]_{\text{dipole}}=-\frac{C_d\alpha_s}{8\pi^2 v}\int d^3k\, d\omega\,\omega\,\text{Im}\left[\frac{1}{k^2\epsilon_L(\omega,k)}+\frac{v^2-\omega^2/k^2}{\omega^2\epsilon_T(\omega,k)-k^2}\right](\mathbf{k}\cdot\mathbf{r}_0)^2\delta(\omega-\mathbf{v}\cdot\mathbf{k}) \tag{4.9}$$

with $C_d=\frac{16}{3}$. It is evident that this stopping power depends on the relative direction of the dipole moment and the motion of the dipole. We can decompose it into scalar and tensor parts:

$$\left[-\frac{dE}{dx}\right]_{\text{dipole}}=S(v)+T(v)[3(\hat{\mathbf{v}}\cdot\hat{\mathbf{d}})^2-1]\,, \tag{4.10}$$

where

$$S(v)=-\frac{C_d\alpha_s r_0^2}{24\pi^2 v}\int d^3k\, d\omega\,\omega k^2\text{Im}\left[\frac{1}{k^2\epsilon_L(\omega,k)}+\frac{v^2-\omega^2/k^2}{\omega^2\epsilon_T(\omega,k)-k^2}\right]\delta(\omega-\mathbf{v}\cdot\mathbf{k})\,, \tag{4.11}$$

$$T(v)=-\frac{C_d\alpha_s r_0^2}{16\pi^2 v}\int d^3k\, d\omega\left[\frac{\omega^2}{v^2}-\frac{k^2}{3}\right]\text{Im}\left[\frac{1}{k^2\epsilon_L(\omega,k)}+\frac{v^2-\omega^2/k^2}{\omega^2\epsilon_T(\omega,k)-k^2}\right]\delta(\omega-\mathbf{v}\cdot\mathbf{k})\,. \tag{4.12}$$

The scalar part of the stopping power gives the average over the direction of the dipole moment with respect to the direction of the motion.

We calculate (4.11) and (4.12) by separating the k integrals into two parts, short-distance ($k>k_0$) and long-distance ($k<k_0$) parts, as done for a single parton. Let us first examine the long-distance part of the dipole stopping power:

$$S_{k<k_0}(v)=-\frac{C_d\alpha_s r_0^2}{12\pi v^2}\int_0^{k_0}dk\,k\int_{-vk}^{vk}d\omega\,\omega\,\text{Im}\left[\frac{1}{\epsilon_L(\omega,k)}+\frac{v^2k^2-\omega^2}{\omega^2\epsilon_T(\omega,k)-k^2}\right]\,, \tag{4.13}$$

$$T_{k<k_0}(v)=-\frac{C_d\alpha_s r_0^2}{8\pi v^2}\int_0^{k_0}dk\frac{1}{k}\int_{-vk}^{vk}d\omega\,\omega\left[\frac{\omega^2}{v^2}-\frac{k^2}{3}\right]\text{Im}\left[\frac{1}{\epsilon_L(\omega,k)}+\frac{v^2k^2-\omega^2}{\omega^2\epsilon_T(\omega,k)-k^2}\right]\,. \tag{4.14}$$

It is easy to see by dimensional analysis that the magnitude of this long-distance part of the color dipole stopping power is given beside some numerical factor by $C_d\alpha_s m_D^4 r_0^2$, which is smaller than the corresponding part of the monopole stopping power by the factor $(m_D r_0)^2$. This reduction is simply due to the color neutrality of the dipole at large distances.

We plot the numerical result of $S_{k<k_0}(v)$ and $T_{k<k_0}(v)$ in Fig. 3 for the cases $k_0=m_D$ and $k_0=2m_D$ (the same cutoffs as Fig. 1) with $r_0=1/2m_D$. (We have implicitly assumed that $r_0<1/m_D$ since, otherwise, the pair cannot form a bound state due to the screening of the binding force [24].) As expected, the magnitude of these long-distance parts of the dipole stopping power is 1 order of magnitude smaller than the same part of the stopping power for a single parton shown in Fig. 1. Note that the tensor part is always positive. This implies that the dipole stopping power is larger when the dipole moment is oriented in the direction of the motion of the pair. We compare in Fig. 4 the dipole stopping power for the two extreme cases $\delta=0$ and $\pi/2$, where δ is the angle of the orientation of the dipole moment with respect to the direction of motion. The reason for this angular dependence of the dipole stopping power may be understood

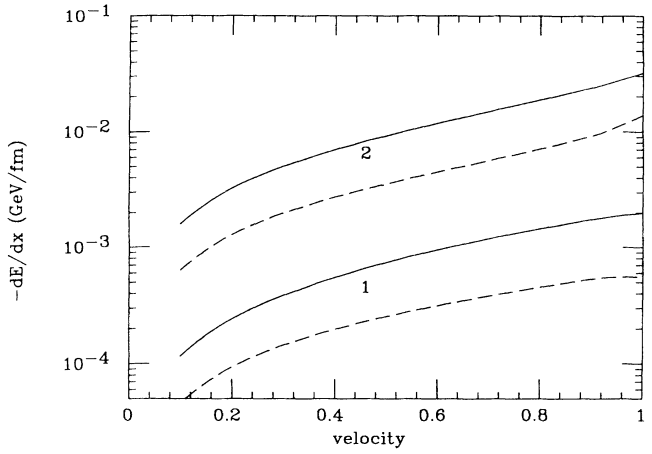

FIG. 3. Dipole contributions to stopping powers for a color-singlet $Q\bar{Q}$ dipole due to the long-range effects using two cutoffs: (1) m_D, (2) $2m_D$. Solid lines are the scalar part $S(v)$ and dashed lines are the tensor part $T(v)$.

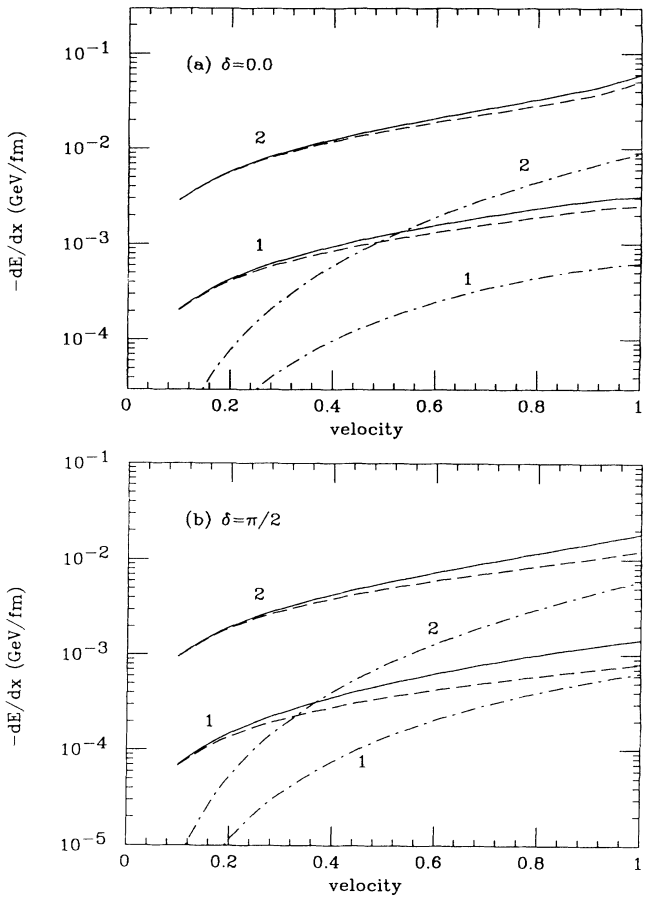

FIG. 4. Stopping power for a color-singlet dipole due to the long-range effects for two relative orientation angles: (a) $\delta=0$, (b) $\delta=\pi/2$. See the caption of Fig. 1 for the meaning of the lines.

intuitively by inspecting the spatial distribution of the energy deposited in the plasma, Eq. (3.11), as plotted in Fig. 5 ($\delta=0$) and Fig. 6 ($\delta=\pi/2$). The pattern of Figs. 5 and 6 can be easily understood by the same consideration as the single parton case. The electric field **E** emanates from Q_1 and sinks into Q_2. $\mathbf{J}_{\rm ind}$ draws similar curves to the case of a single parton due to the presence of the incoming $Q\bar{Q}$. Therefore, the induced current $\mathbf{J}_{\rm ind}$ has more parallel components with **E** in the longitudinal case ($\delta=0$) than the orthogonal case ($\delta=\pi/2$). In the former case, the region of positive-energy deposition ($d^4W/dtd^3r>0$) extends even more in the longitudinal direction compared with the case of single test charge (recall Fig. 2). Actually, the flow pattern of $\mathbf{J}_{\rm ind}$ receives some superposition of the component moving along **E** onto the above "removal-return" pattern, so the energy-deposition pattern gets more complicated in the orthogonal case. From Figs. 5 and 6, we can see that the region in which $d^4W/dt\,d^3r>0$ is wider in the longitudinal case than in the orthogonal case, and hence the former undergoes a larger stopping power. As a whole, the energy supplied by test charges (both a single charge and a pair) is distributed more in the transverse direction than in the longitudinal direction with respect to the velocity of the test charges, especially when the velocity becomes larger. From this fact one may say that the screening effect for a pair is larger in the transverse case than the longitudinal case, and hence the larger stopping power for the latter.

The short-distance part can be evaluated in the same way as we have done in (3.5) for a single test charge:

$$S_{k>k_0}(v)\simeq\frac{C_d\alpha_s m_D^2 r_0^2}{48\pi v}\int_{k>k_0}d^3k\,d\omega\,k\omega^2\left[\frac{1}{k^4}-\frac{v^2-\omega^2/k^2}{2k^2(\omega^2-k^2)}\right]\delta(\omega-\mathbf{v}\cdot\mathbf{k})$$
$$=\frac{C_d\alpha_s m_D^2 r_0^2}{24}\frac{1}{v^2}\left[v+\frac{1-v^2}{2}\ln\left[\frac{1-v}{1+v}\right]\right]\int_{k_0}dk\,k\ , \tag{4.15}$$

$$T_{k>k_0}(v)\simeq\frac{C_d\alpha_s m_D^2 r_0^2}{32\pi v}\int_{k>k_0}d^3k\,d\omega\frac{\omega^2}{k}\left[\frac{\omega^2}{v^2}-\frac{k^2}{3}\right]\left[\frac{1}{k^4}-\frac{v^2-\omega^2/k^2}{2k^2(\omega^2-k^2)}\right]\delta(\omega-\mathbf{v}\cdot\mathbf{k})$$
$$=\frac{C_d\alpha_s m_D^2 r_0^2}{16}\frac{1}{v^4}\left[\frac{4}{15}v^5-v^3+v+\frac{(1-v^2)(3-v^2)}{6}\ln\left[\frac{1-v}{1+v}\right]\right]\int_{k_0}dk\,k\ . \tag{4.16}$$

These integrals suffer a more severe (quadratic) divergence in the ultraviolet region than that in (3.5). There are now two physical conditions which set the upper limit on the k integral: (i) a constraint on the maximum momentum transfer by two-body collision kinematics [$k < k_{\max} = 2T(E+T)/(E-p+2T)$] ($p$ is the momentum of the parton; see the Appendix for details), and (ii) the condition for the convergence of the multipole expansion ($k < 1/r_0$). When $k_{\max} \ll 1/r_0$, condition (i) becomes stronger; therefore,

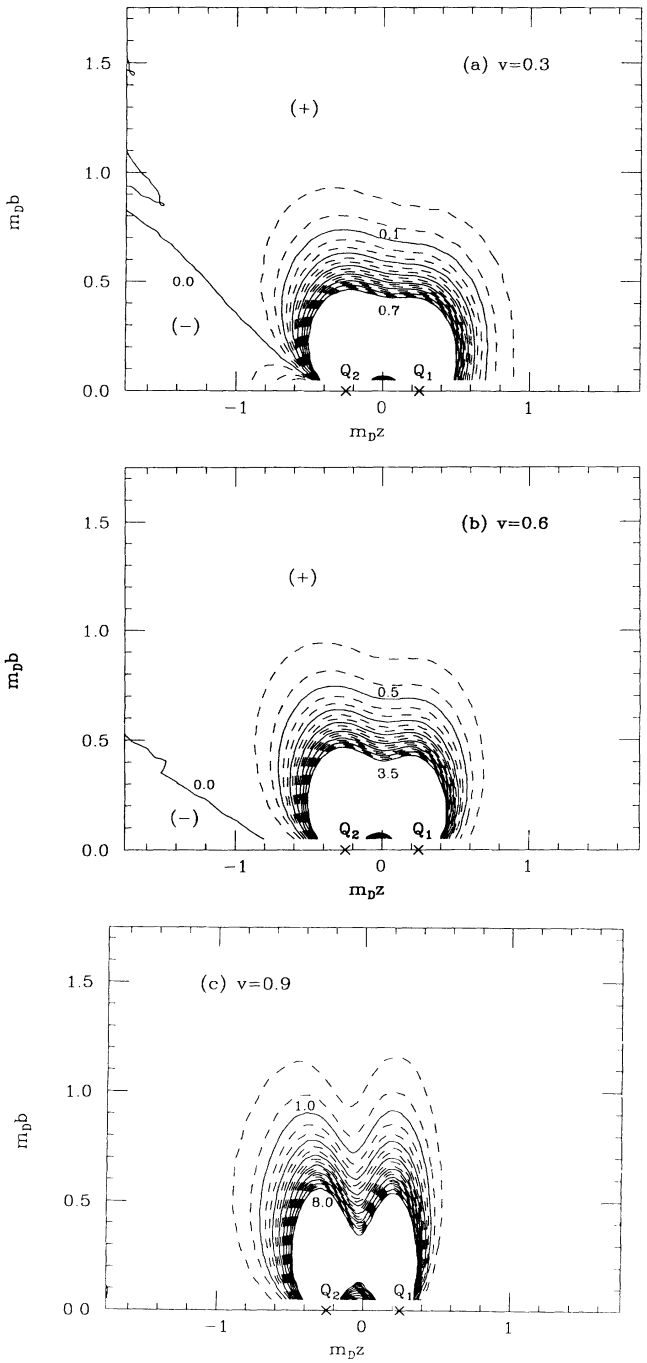

FIG. 5. Contour plots of the distribution of the energy supplied to the plasma by a longitudinally aligned ($\delta=0$) color-singlet dipole per unit time for three velocities of the dipole: (a) $v=0.3$, (b) $v=0.6$, (c) $v=0.9$. Q_1 and Q_2 denote the positions of the two charges composing the dipole. See the caption to Fig. 2.

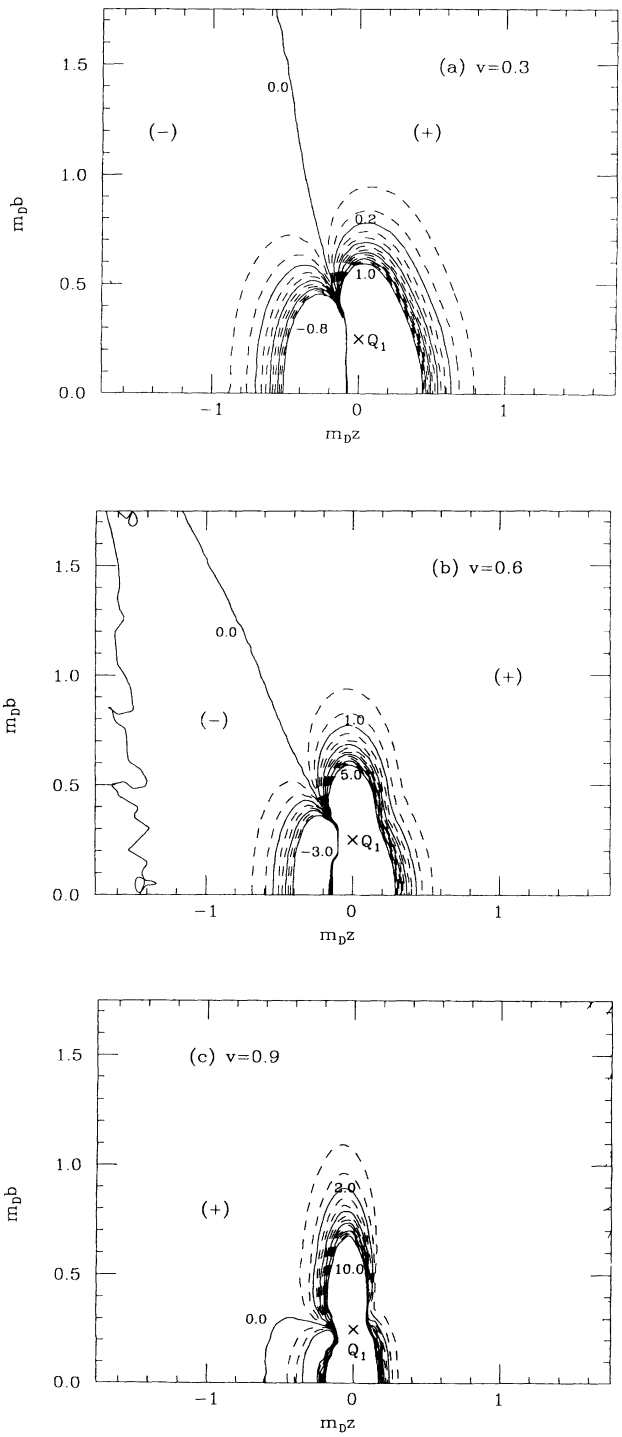

FIG. 6. The same as Fig. 5 but for the orthogonal case ($\delta=\pi/2$). See the caption of Fig. 5.

$$S_{k>k_0}(v)\simeq\frac{C_d\alpha_s m_D^2(r_0k_{\max})^2}{48}\frac{1}{v^2}\left[v+\frac{1-v^2}{2}\ln\left[\frac{1-v}{1+v}\right]\right], \tag{4.17}$$

$$T_{k>k_0}(v)\simeq\frac{C_d\alpha_s m_D^2(r_0k_{\max})^2}{32}\frac{1}{v^4}\left[\frac{4}{15}v^5-v^3+v+\frac{(1-v^2)(3-v^2)}{6}\ln\left[\frac{1-v}{1+v}\right]\right], \tag{4.18}$$

where we assumed $k_{\max}\gg k_0$. As we see, in this case the multipole expansion of the stopping power becomes the expansion in (even) powers of $k_{\max}r_0(\ll 1)$. From Eq. (4.18), we can see that the tensor part is positive, $T_{k>k_0}(v)>0$, as we interpreted from Figs. 5 and 6 in the previous paragraph.

On the other hand, if $k_{\max}\gg 1/r_0$, then one would rather like to take the ultraviolet cutoff at $k\sim 1/r_0$. This procedure would make both $S_{k>k_0}(v)$ and $T_{k>k_0}(v)$ independent of r_0. This signifies the breakdown of the multipole expansion. In this case, all higher multipoles give the same order-of-magnitude contribution to the stopping power and therefore the sum of the entire series is required. It is not difficult to find the limiting behavior of this sum. The exact form of the stopping power for a pair of changes can be obtained from

$$\begin{aligned}\left[-\frac{dE}{dx}\right]_{\text{pair}}&=-Q_1\frac{\mathbf{v}}{v}\cdot\mathbf{E}^{(\text{pair})}\left[\frac{\mathbf{r}_0}{2}+\mathbf{v}t,t\right]-Q_2\frac{\mathbf{v}}{2}\cdot\mathbf{E}^{(\text{pair})}\left[-\frac{\mathbf{r}_0}{2}+\mathbf{v}t,t\right]\\&=-\frac{1}{(2\pi)^3v}\int d^3k\,d\omega\,\omega\,\text{Im}\left[\frac{1}{k^2\epsilon_L(\omega,k)}+\frac{v^2-\omega^2/k^2}{\omega^2\epsilon_T(\omega,k)-k^2}\right]\left[Q_1\exp\left[-\frac{i}{2}\mathbf{k}\cdot\mathbf{r}_0\right]+Q_2\exp\left[\frac{i}{2}\mathbf{k}\cdot\mathbf{r}_0\right]\right]\\&\quad\times\left[Q_1\exp\left[\frac{i}{2}\mathbf{k}\cdot\mathbf{r}_0\right]+Q_2\exp\left[-\frac{i}{2}\mathbf{k}\cdot\mathbf{r}_0\right]\right]\delta(\omega-\mathbf{v}\cdot\mathbf{k})\\&=-\frac{1}{(2\pi)^3v}\int d^3k\,d\omega\,\omega\,\text{Im}\left[\frac{1}{k^2\epsilon_L(\omega,k)}+\frac{v^2-\omega^2/k^2}{\omega^2\epsilon_T(\omega,k)-k^2}\right]\\&\quad\times(Q_1^2+Q_2^2+Q_1Q_2e^{-i\mathbf{k}\cdot\mathbf{r}_0}+Q_2Q_1e^{i\mathbf{k}\cdot\mathbf{r}_0})\delta(\omega-\mathbf{v}\cdot\mathbf{k})\,.\end{aligned} \tag{4.19}$$

At large k ($\gg 1/r_0$), the last two "interference" terms in the small parentheses oscillate rapidly so that the integration of these terms cancel out in the short-wavelength region. The remnant is a simple incoherent sum of the stopping power on two individual charges Q_1 and Q_2:

$$\left[-\frac{dE}{dx}\right]_{\text{pair}}^{k>k_0}=\frac{(C_{Q_1}+C_{Q_2})\alpha_s m_D^2}{2}\frac{1}{v^2}\times\left[v+\frac{1-v^2}{2}\ln\left[\frac{1-v}{1+v}\right]\right]\ln\left[\frac{p}{k_0}\right]. \tag{4.20}$$

Thus, the energy loss of a color-neutral pair of partons becomes of the same order of magnitude as that of a single color charge as long as the pair momentum becomes greater than the inverse size of the pair. These short-distance incoherent collisions naturally involve large momentum transfer to individual components of the pair and therefore work to disrupt the coherent motion of the pair, resulting in the suppression of the bound-state formation from these pairs. What is calculated here is the loss of the energy associated with the center-of-mass motion of the pair without referring to the change of its relative motion energy.

This result may first appear to contradict with the "color transparency" effect [25] that the plasma medium becomes transparent for a color-singlet pair at sufficiently high energies. To avoid possible confusion, we note that the absence of the color transparency here is merely due to the condition that the pair size is greater than the inverse momentum of the pair. Actually, in a real physical situation, the pair is created initially with a very small mutual separation which is of order of the inverse momentum of the pair by the uncertainty principle and this distance will remain small for high-energy pairs due to the Lorentz time dilatation unless the pair traverses in the plasma for a very long time. Therefore, we expect that high-energy pairs created in the collision will escape the plasma of finite space-time extension without suffering much from the energy loss and the suppression of the bound-state formation heals for the high-energy pair. An estimate of these effects on the spectrum of the charmonium requires a more dynamical treatment of the plasma evolution, which is out of the scope of the present study.

V. SUMMARY AND CONCLUSIONS

In this paper we have studied the energy-loss mechanism of partons traversing a quark-gluon plasma in terms of the semiclassical kinetic theory. The energy-loss formulas which embody the screening of the long-range part of the interactions were derived and examined by the standard kinetic method which describes the plasma as a

continuous dielectric media in terms of the collisionless Boltzmann-Vlasov equation. Our result for a single parton in homogeneous equilibrium plasmas essentially agrees with that of Thoma and Gyulassy. We have applied this method also to compute the energy loss of a pair of partons in equilibrium plasmas. We recapitulate our result.

(1) In the case of a single parton, the short-range part of the interaction gives a much bigger contribution to the energy loss than the long-range part, which is screened by the plasma collective response. The logarithmic infrared divergence, which would appear in the bare one-gluon-exchange interactions, is removed by the dynamic screening. The logarithmic ultraviolet divergence, which arises due to the neglect of recoil in the two-body collision kinematics at short distances in our treatment, is removed by introducing a cutoff at the maximum momentum transfer allowed in the collision. This procedure gives approximately (within 10%) the same stopping power given by a microscopic Feynman-diagram calculation [9]. At very high energy, the stopping power shows the logarithmic energy dependence. We showed that the region where the energy is deposited depends strongly on the velocity of the test charge. As the velocity increases the energy is deposited more in the transversely extended region reflecting the Lorentz contraction of the induced field. We note that there appears no singular behavior in either the induced field or the pattern of the energy distribution, as already anticipated by the absence of the collective excitation in the energy transfer.

(2) The energy loss of a color-singlet dipole depends strongly on the ratio of the size of the pair and the inverse of its net momentum. When this ratio is small, the dipole stopping power is weakened substantially compared to the stopping power for the single test charge as expected from the overall color neutrality of the pair, while in the other case the dipole stopping power becomes essentially dominated by the short-range (unscreened) part of the interactions and, consequently, it becomes comparable to the stopping power for the single test charge. Although relatively weak compared with the absolute strength, the dipole stopping power depends on the orientation of the pair with respect to the direction of the motion and the alignment in the direction of the motion is favored for effective energy deposition.

(3) Numerically, our estimate of the energy loss gives $(-dE/dx)\sim 0.4-1.0$ GeV/fm both for a single parton and a color dipole with an energy ~ 10 GeV near the deconfinement transition temperature and its precise value is very sensitive to the value of the screening mass. These values are comparable to that of the hadronic string tension (~ 1 GeV/fm), which gives the scale of the energy loss per unit length of colored parton(s) in a confining QCD vacuum.

The mechanism of the energy deposition studied in the present paper is *adiabatic,* namely, it does not involve the increase of entropy in the plasma and thus our method does not describe the thermalization of the energy deposited by the high-energy partons. This is a direct consequence of our neglect of the collision term in solving the Boltzmann-Vlasov equation. This approximation is equivalent to the neglect of statistical fluctuations in the microscopic distribution of the plasma constituents and the local field. Although this approximation may be well justified for ordinary nonrelativistic plasmas, it is only marginal in the case of the quark-gluon plasma [26]. It thus deserves further study to refine our present calculation by the inclusion of the collision term. It is also important to incorporate the inelastic collisions (bremsstrahlung and pair creation) which are expected to dominate at high energies [27].

ACKNOWLEDGMENTS

We thank Miklos Gyulassy for very informative communications. One of us (Y.K.) also thanks Berndt Müller and Stephen Wallace for useful conversations. This work was supported in part by funds provided by the U.S. Department of Energy (DOE) under Contract Nos. DE-FG05-87ER-40322, DE-AC02-76ER03069, and DE-FG02-87ER40365.

APPENDIX

In our whole discussion about the stopping power based on kinetic theory, we completely neglected the recoils of both the incident external parton and the scattered plasma constituents. The neglect of the recoils of the plasma constituents leads to the logarithmic divergence in the expression for the stopping power. If we derived the stopping power starting from the microscopic Feynman diagram as is done by Braaten and Thoma [9], we could automatically get the kinematic constraint which determines the momentum cutoff in the expression of the stopping power. The momentum dependence of the stopping power is, however, at most, logarithmic, and therefore, by taking into account the kinematic constraint as the form of the momentum integral cutoff, we can reproduce the results of the stopping power in the microscopic derivation by our simple kinetic theory approach except small correction factors. In this appendix we summarize the kinematics of the two-body collision relevant to our study.

Suppose an external parton with mass M and four-momentum $P=(E,\mathbf{p})$ $(E=\sqrt{M^2+\mathbf{p}^2})$ has an elastic collision with a massless plasma constituent with the four-momentum $Q=(q,\mathbf{q})$ $(q=|\mathbf{q}|)$ and their momenta, respectively, become $P'=(E',\mathbf{p}')$ $(E'=\sqrt{M^2+\mathbf{p}'^2})$ and $Q'=(q',\mathbf{q}')$ $(q'=|\mathbf{q}'|)$. The energy and momentum transfers are, respectively, $\omega=E-E'=q'-q$ and $\mathbf{k}=\mathbf{p}-\mathbf{p}'=\mathbf{q}'-\mathbf{q}$ by the conservation of four-momentum. From the relation $\mathbf{k}=\mathbf{q}'-\mathbf{q}$ and $\omega=q'-q$, we get

$$|\omega|=|q-q'|\le k=|\mathbf{k}|\le q+q'=2q+\omega\ . \tag{A1}$$

On the other hand, from $\omega=E-E'=E-\sqrt{M^2+(\mathbf{p}-\mathbf{k})^2}=E-\sqrt{E^2+k^2-2\mathbf{p}\cdot\mathbf{k}}$ we get the relation

$$-2pk+k^2\le\omega^2-2\omega E\le 2pk+k^2\ , \tag{A2}$$

where $p=|\mathbf{p}|$. From Eqs. (A1), (A2), and the condition $p\gg\omega,q$, we get the following constraint for ω:

$$\frac{-2q(p+q)}{E+p+2q} \le \omega \le \frac{2q(p-q)}{E-p+2q} . \tag{A3}$$

It follows from this equation and Eq. (A1) $k \le \omega + 2q$ that

$$k \le \frac{2q(E+q)}{E-p+2q} = \frac{2q(1+q/E)}{1-v+2q/E} , \tag{A4}$$

where $v = p/E$ is the velocity of the external parton. Condition (A4) can be simplified in several limits. For this purpose we note the denominator of Eq. (A4) can be estimated as

$$1-v = \frac{1-v^2}{1+v} = \frac{1}{1+v}\left[\frac{M}{E}\right]^2 \sim \left[\frac{M}{E}\right]^2, \quad \frac{q}{E} \sim \frac{T}{E} . \tag{A5}$$

Therefore, we can approximate condition (A4) in two limits. If $1 \gg T/E \gg (M/E)^2$, i.e., $E \gg T$ and $E \gg M^2/T$, then

$$k \le E . \tag{A6}$$

If $1 \gg (M/E)^2 \gg T/E$, i.e., $T \ll M \ll E \ll M^2/T$, then

$$k \le \frac{2q}{1-v} \sim \frac{2T}{1-v} . \tag{A7}$$

For the massless quark ($E = p$), conditions (A3) and (A4) become

$$-q \le \omega \le p-q, \quad k \le p+q . \tag{A8}$$

In our kinetic theory calculation, the condition $\omega = \mathbf{v}\cdot\mathbf{k}$ appeared from the beginning corresponding to the straight path approximation for the external parton. This approximation is allowed when $E \gg T$ as is seen from the relation

$$\omega = E - \sqrt{E^2+k^2-2E\mathbf{v}\cdot\mathbf{k}} = \mathbf{v}\cdot\mathbf{k} + EO\left[\left[\frac{T}{E}\right]^2\right] . \tag{A9}$$

[1] J. D. Jackson, *Classical Electrodynamics,* 2nd ed. (Wiley, New York, 1975), Chap. 13.

[2] L. D. Landau, E. M. Lifshitz, and L. P. Pitaevskii, *Electrodynamics of Continuous Media,* 2nd ed. (Pergamon, New York, 1984), Chap. 14.

[3] S. Ichimaru, *Basic Principles of Plasma Physics* (Benjamin, Reading, 1973).

[4] J. D. Bjorken, Fermilab Report No. Pub-82/59-THY, 1982 (unpublished), and erratum.

[5] D. A. Appel, Phys. Rev. D **33**, 717 (1986).

[6] J.-P. Blaizot and L. McLerran, Phys. Rev. D **34**, 2739 (1986).

[7] M. Gyulassy and M. Plümer, Phys. Lett. B **243**, 432 (1990).

[8] M. H. Thoma and M. Gyulassy, Nucl. Phys. **B351**, 491 (1991); see also, S. Mrówczyński, Phys. Lett. B **269**, 383 (1991).

[9] E. Braaten and M. H. Thoma, Phys. Rev. D **44**, 1298 (1991); **44**, 2625 (1991); M. H. Thoma, Phys. Lett. B **273**, 128 (1991).

[10] K. J. Eskola, K. Kajantie, and J. Lindfors, Nucl. Phys. **B323**, 37 (1989).

[11] M.-C. Chu and T. Matsui, Phys. Rev. D **39**, 1892 (1989).

[12] J. D. Bjorken, Phys. Rev. D **27**, 140 (1983).

[13] H. T. Elze and U. Heinz, Phys. Rep. **183**, 81 (1989).

[14] V. V. Klimov, Zh. Eksp. Teor. Fiz. **82**, 336 (1982) [Sov. Phys. JETP **55**, 199 (1982)].

[15] H. A. Weldon, Phys. Rev. D **26**, 1394 (1982).

[16] K. Kajantie and J. Kapusta, Ann. Phys. (N.Y.) **160**, 477 (1985).

[17] E. Braaten and R. D. Pisarski, Phys. Rev. Lett. **64**, 1338 (1990); Nucl. Phys. **B337**, 569 (1990); J. Frenkel and J. C. Taylor, *ibid.* **B334**, 199 (1990); R. Kobes, G. Kunstatter, and A. Rebhan, Phys. Rev. Lett. **64**, 2992 (1990).

[18] The friction force on a heavy quark has been computed by Svetitsky in the Landau diffusion approximation for the lowest-order QCD collision integral: B. Svetitsky, Phys. Rev. D **37**, 2484 (1988).

[19] The definition of the dielectric function is not unique, although the number of the independent scalar functions is two. For example, instead of the combination (ϵ_L, ϵ_T), the following electric permittivity $\epsilon(\omega,k)$ and the magnetic permiability $\mu(\omega,k)$ are sometimes used: $\epsilon(\omega,k) = \epsilon_L(\omega k)$, $1/\mu(\omega,k) = 1+(\omega/k)^2[\epsilon_L(\omega,k) - \epsilon_T(\omega,k)]$, with an appropriate modification in Eqs. (2.8)–(2.11) (see Ref. [3] for more detail).

[20] E. M. Lifshitz and L. P. Pitaevskii, *Physical Kinetics* (Pergamon, New York, 1981).

[21] For the recent result of the numerical simulation of QCD on a lattice see, for example, A. Ukawa, in *Non-Perturbative Aspects of the Standard Model,* Proceedings, Jara, Spain, 1988, edited by J. Abad, M. B. Gavela, and A. Gonzalez-Arroyo [Nucl. Phys. B (Proc. Suppl.) **10A**, 66 (1989)].

[22] M. Gao, Phys. Rev. D **41**, 626 (1990); F. Karsch, in *Lattice '88,* Proceedings of the International Symposium, Batavia, Illinois, 1988, edited by A. S. Kronfeld and P. B. Mackenzie [Nucl. Phys. B (Proc. Suppl.) **9**, 357 (1989)].

[23] T. Matsui, Phys. Lett. **132B**, 260 (1983).

[24] T. Matsui and H. Satz, Phys. Lett. B **178**, 416 (1986).

[25] A. H. Mueller, in *Proceedings of the XVIIth Rencontre de Moriond: II. Elementary Hadronic Processes and New Spectroscopy,* Les Arcs, France, 1982, edited by J. Tran Thanh Van (Editions Frontieres, Gif-sur-Yvette, 1982); G. Bertsch, S. J. Brodsky, A. S. Goldhaber, and J. G. Gunion, Phys. Rev. Lett. **47**, 297 (1981); G. R. Farrar, H. Liu, L. L. Frankfurt, and M. I. Strikman, *ibid.* **61**, 686 (1988).

[26] In the nonrelativistic kinetic theory of ordinary plasmas, this approximation is justified on the basis of the smallness of the so-called plasma parameter defined by $g_{\rm pl} = m_D^3/n$, where n is the number density of the plasma constituents and m_D is the Debye screening mass. This parameter measures the relative significance of the individual particle behavior of the plasma with respect to its collective behavior as a continuous medium. Since the plasma parameter is proportional to the ratio of the average interaction ener-

gy and the average kinetic energy of plasma constituents, it becomes small at sufficiently high temperatures provided that the temperature is still much smaller than the mass m of the plasma constituents. The collision term describes the higher-order effect in terms of $g_{\rm pl}$ and hence may be neglected. For relativistic plasmas where $T \gg m$, the plasma parameter is reduced to $g_{\rm pl} \simeq \alpha^{3/2}$ so that the collision term describes the higher-order effect in the ordinary sense of the perturbation in the coupling strength.

[27] A. H. Sorensen, Duke University Report No. Duke-TH91/14, 1991 (unpublished); M. Gyulassy, M. Plumer, M. Thoma, and X. N. Wang, Proceedings of Intersections between Particle and Nuclear Physics, Tucson, AZ, 1991 (unpublished), p. 224.